

Homogeneity of Phytochrome Cph1 Vibronic Absorption Revealed by Resonance Raman Intensity Analysis

Katelyn M. Spillane,[†] Jyotishman Dasgupta,[†] J. Clark Lagarias,[‡] and Richard A. Mathies^{*,†}

Department of Chemistry, University of California, Berkeley, California 94720, and Department of Molecular and Cellular Biology, University of California, Davis, California 95616

Received July 14, 2009; E-mail: ramathies@berkeley.edu

Phytochromes are a family of photoreceptors found in plants, bacteria, and fungi that act as light-activated biological switches. They utilize covalently bound bilin chromophores that interconvert between two spectrally distinct conformers, a red (P_r) and far-red (P_{fr}) light-absorbing form,¹ to drive signal transduction that ultimately controls growth and development.² The phototransformation is both rapid and reversible and is driven by a *Z*-to-*E* isomerization about the $C_{15}=C_{16}$ methine bridge between the C and D rings of the linear tetrapyrrole chromophore (see Figure 1).^{1,3} However, the molecular structural evolution along the P_r -to- P_{fr} reaction coordinate is not yet fully understood.

Ultrafast transient absorption measurements on the cyanobacterial phytochrome Cph1, the plant phytochrome phyA, and the bacteriophytochrome Agp1 have been used to characterize the electronic changes in the P_r -to- P_{fr} transition.^{4–7} These studies revealed two excited-state lifetimes characterized by a short (5–16 ps) and a long (25–40 ps) time constant, indicating at least two P_r excited states, but it is unknown whether these multiple states originate from a heterogeneous ground-state population or multiple reaction intermediates formed from a single initial conformer. The shape of the absorption band ($\lambda_{max} = 660$ nm), which features a distinct shoulder on the blue edge at ~ 620 nm (see Figure 1), has also attracted attention and has been interpreted by many as evidence for conformational heterogeneity of the ground state bilin chromophore population.^{8–10} Resolution of the ground-state bilin conformer population is of fundamental importance in elucidating the excited-state reaction pathway and ultimately the cause of the low 15% photoisomerization quantum yield.¹¹

Here we investigate the P_r ground state of the cyanobacterial phytochrome Cph1 chromophore using resonance Raman intensity analysis to calculate the vibronic absorption profile. Measured resonance Raman intensities can be used to quantify the individual vibronic displacements that make up the Franck–Condon vibronic absorption spectrum. In this paper, we show that the absorption band profile including the prominent blue shoulder is due simply to vibronic transitions resulting from the absorption of a single P_r conformer of Cph1.

Recombinant Cph1 phytochrome (N514) was expressed and purified as described previously.¹² Prior to spectroscopic studies, samples were dialyzed against 1 L of buffer (25 mM TES-KOH, pH 8.0, 25 mM KCl, 10% glycerol) and then concentrated to 10.6 OD₆₆₀/cm. For absolute Raman cross section calibration, a standard solution of NaNO₃ (250 mM) was used. The protein sample for measurement contained 1.25×10^{-4} M Cph1 in glycerol-containing TES buffer. The stimulated Raman spectrum was obtained using the experimental setup described by McCamant et al.¹⁴ (see Supporting Information (SI)).

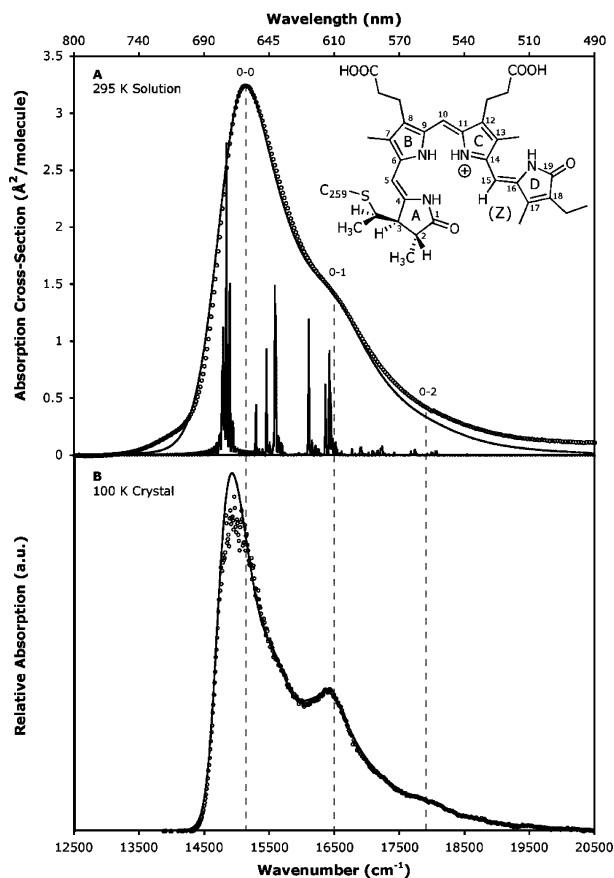


Figure 1. Comparison of the experimental and calculated absorption spectra for the P_r form of phytochrome Cph1 at 295 K in solution (A) and at 100 K in crystalline form (B).¹³ Experimental absorption spectra are shown as open circles. Calculated absorption spectra are shown as solid lines and were determined using the parameters listed in Table 1. The absorption FC factors for all modes with $\Delta > 0.2$ are presented (0–0 transition scaled $\times 0.0025$) (see Supporting Information (SI)) (A). The ground state chromophore structure in the P_r form is ZZZssa as shown.

The absolute Raman cross sections of Cph1 were determined as described previously.¹⁵ Briefly, the differential cross sections of the Cph1 bands were calculated using the 1049 cm^{-1} glycerol C–OH stretch mode as an internal standard. The absolute Raman cross sections were determined from eq 1:

$$\sigma_{\text{Cph1}} = \frac{8\pi(1 + 2\rho)}{3(1 + \rho)} \left(\frac{\partial \sigma}{\partial \Omega} \right)_{\text{Cph1}} \quad (1)$$

where the depolarization ratios, ρ , for all Cph1 bands were measured and found to be $\sim 1/3$.

Raman excitation profiles (REPs) were calculated using the time-dependent wavepacket formalism of resonance Raman scattering.¹⁶

[†] University of California, Berkeley.

[‡] University of California, Davis.

Table 1. Resonance Raman Cross Sections of Cph1 (P_r)

frequency [cm^{-1}]	expt cross section [$\text{\AA}^2 \times 10^{-11}$] ^a	calcd cross section [$\text{\AA}^2 \times 10^{-11}$]	delta [unitless] ^b
50	—	—	0.80
502	3.11 ± 0.71	2.82	0.22
664	7.77 ± 1.39	7.44	0.29
722	1.05 ± 0.71	0.81	0.09
793	13.9 ± 2.38	13.9	0.35 (0.34)
808	11.9 ± 2.12	11.9	0.32 (0.31)
859	2.84 ± 0.63	2.83	0.15
892	0.73 ± 0.91	0.65	0.07
906	0.97 ± 0.79	0.86	0.08
967	1.69 ± 0.59	1.46	0.10
1116	1.54 ± 0.54	1.40	0.09
1204	2.34 ± 0.82	2.27	0.11
1225	6.26 ± 2.63	6.19	0.18
1235	4.84 ± 1.81	4.93	0.16
1301	6.40 ± 2.52	4.57	0.15
1314	20.0 ± 5.07	19.7	0.31 (0.37)
1331	5.44 ± 1.69	4.08	0.14
1379	2.27 ± 0.61	2.15	0.10
1456	2.17 ± 1.71	1.84	0.09
1474	4.26 ± 3.15	4.49	0.14
1530	1.81 ± 0.53	1.92	0.09
1569	12.4 ± 2.09	12.3	0.23 (0.25)
1630	24.8 ± 4.10	24.8	0.32 (0.35)
1652	12.9 ± 2.29	12.8	0.23 (0.25)

^a Resonance Raman cross sections for the P_r form of phytochrome Cph1 determined relative to the 1049 cm^{-1} C—OH stretch of glycerol. The glycerol differential cross section at $\lambda_{\text{ex}} = 790.4 \text{ nm}$ was $5.28 \times 10^{-16} \text{ \AA}^2 \text{ molecule}^{-1}$. ^b Delta values for the room temperature structure were determined from Raman intensity calculations with $\Gamma = 880 \text{ cm}^{-1}$, $\theta = 90 \text{ cm}^{-1}$, $E_0 = 14800 \text{ cm}^{-1}$, and $M = 2.32 \text{ \AA}$. Delta values for the crystal structure were determined using $\Gamma = 430 \text{ cm}^{-1}$, $\theta = 50 \text{ cm}^{-1}$, $E_0 = 14690 \text{ cm}^{-1}$, and $M = 2.32 \text{ \AA}$ and are shown in parentheses when different from the room temperature values.

The absorption cross sections, σ_A , were determined by the Fourier transform of $\langle ili(t) \rangle$, where $|i\rangle$ is the initial vibrational eigenstate on the ground electronic surface and $|l\rangle$ is the vibrational wave function of the initial state propagating on the excited electronic surface. The Raman cross sections, σ_R , were determined by the square of the half-Fourier transform of $\langle fli(t) \rangle$, where $|f\rangle$ is the final vibrational eigenstate on the ground electronic surface (see SI). The time-dependent overlaps, $\langle ili(t) \rangle$ and $\langle fli(t) \rangle$, depend on the dimensionless parameter Δ , which is the displacement between the ground and excited electronic state harmonic minima. Relative delta values were initially estimated from the intensities of the observed vibrational bands assuming $I \propto \omega^2 \Delta^2$.¹⁷ The overall scaling of Δ , homogeneous broadening Γ_G , inhomogeneous broadening θ , zero—zero transition energy E_0 , and electronic transition length M were then adjusted to provide the best fits.

The experimental and calculated absorption spectra of P_r in solution (295 K) are presented in Figure 1A. The absorption cross section is $3.25 \text{ \AA}^2/\text{molecule}$ at the maximum, which was calculated based on the molar extinction coefficient $\epsilon_{660} = 85000 \text{ M}^{-1} \text{ cm}^{-1}$.¹⁸ The spectrum is dominated by the 0—0 vibronic transition and features a shoulder on the blue edge near 16500 cm^{-1} , which is shown here to be the 0—1 vibronic transition. The absorption profile calculated using parameters derived from a 24-mode Raman intensity vibronic analysis (summarized in Table 1) agrees very well with the experimental spectrum. These parameters include an inhomogeneous broadening of 90 cm^{-1} , a homogeneous broadening of 880 cm^{-1} , and a zero—zero transition energy of 14800 cm^{-1} . The minor baseline difference to the blue of 17250 cm^{-1} is attributed to a weak transition between the Q_y band and the Soret band at 360 nm that was not taken into account in the calculations^{19,20} (see SI Figure S1).

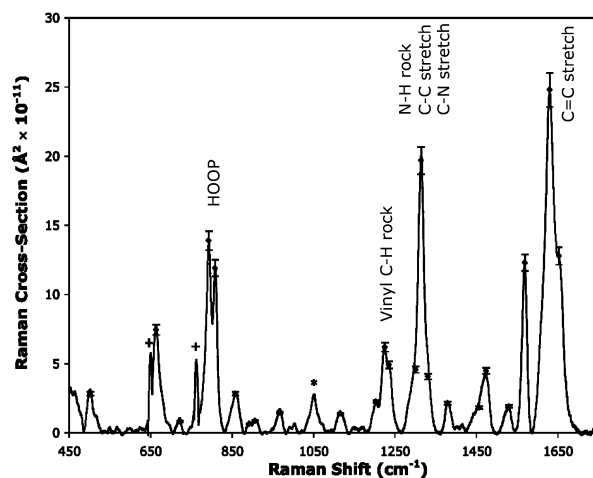


Figure 2. Stimulated Raman spectrum (solid line) of $1.25 \times 10^{-4} \text{ M}$ Cph1 P_r phytochrome obtained using a $3 \mu\text{J}$ Raman pump pulse centered at 790.4 nm . Integrated peak areas were used to determine the absolute Raman cross sections presented in Table 1 using the symmetric stretch of NO_3^- at 1045 cm^{-1} as an external standard. The peak at 1049 cm^{-1} indicated by an * is due to the glycerol internal standard, and the features at 650 and 760 cm^{-1} indicated by a + are detector artifacts.

The slight difference to the red of 14375 cm^{-1} is attributed to a population of vibrational modes with energies below $k_B T$ ($\sim 200 \text{ cm}^{-1}$ at RT) that was not observed experimentally and accounts for less than 5% of the total integrated area. A highly displaced, 50 cm^{-1} mode was included in the calculations to model motion along these missing torsional coordinates.

The experimental and calculated absorption spectra of the crystalline (100 K) form of P_r are also in excellent agreement (Figure 1B). They exhibit the same vibronic features as the solution spectra, evidencing a single chromophore structure. The vibronic transitions are red-shifted by $\sim 100 \text{ cm}^{-1}$ relative to those in solution, most likely due to increased density, polarization, and dispersion interactions. In addition, the decreased temperature changes the distribution of transition energies of the individual molecules, thus reducing the overall line broadening and increasing the prominence of the 0—1 vibronic feature.^{21–23} The parameters that gave the best fit to the 100 K absorption spectrum were an inhomogeneous broadening of 50 cm^{-1} , a homogeneous broadening of 430 cm^{-1} , and a zero—zero transition energy of 14690 cm^{-1} . The molar extinction coefficient of the crystal structure was not determined, and so the spectrum was scaled such that the electronic transition length matched that of the solution structure ($M \approx 2.32 \text{ \AA}$).

The Raman spectrum and calculated Raman cross sections of P_r in solution are presented in Figure 2. Experimental cross sections range from $(0.73 \pm 0.91) \times 10^{-11}$ to $(24.8 \pm 4.10) \times 10^{-11} \text{ \AA}^2 \text{ molecule}^{-1}$ at 892 cm^{-1} and 1630 cm^{-1} , respectively, and were determined by comparison of the P_r integrated peak areas to the integrated area of the glycerol C—OH stretch band at 1049 cm^{-1} . Calculated cross sections were obtained by adjusting the overall scaling of the delta values to match the experimental peak intensities. The most notable bands are the C_{15} —H hydrogen out-of-plane (HOOP) mode at 793 cm^{-1} ($\Delta = 0.35$), the mixture of the C_5 —H and C_{15} —H HOOP modes at 808 cm^{-1} ($\Delta = 0.32$), the N—H in-plane rock at 1314 cm^{-1} ($\Delta = 0.31$), and the C=C stretch at 1630 cm^{-1} ($\Delta = 0.32$) with cross sections on the order of $10^{-10} \text{ \AA}^2/\text{molecule}$ (see Table 1). The equality of delta values indicates that the excitation energy is dissipated among multiple displaced modes as opposed to being focused along a small number of normal

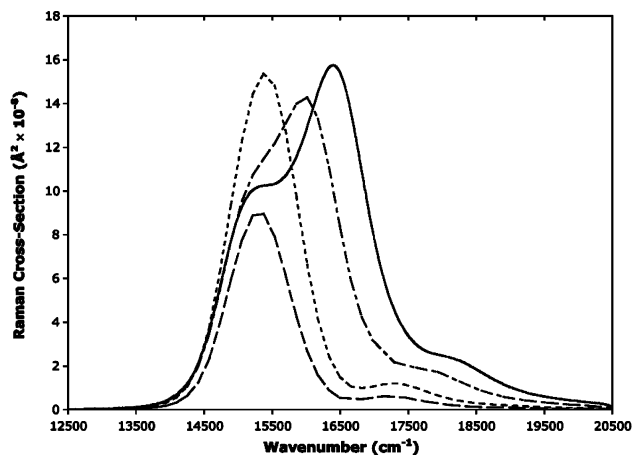


Figure 3. Comparison of representative calculated Raman excitation profiles for the 664 (---), 793 (•••), 1314 (-•-), and 1630 cm^{-1} (-) modes using the parameters listed in Table 1.

coordinates. Therefore, the wavepacket dynamics evidence multimodal evolution along the reaction trajectory.

Raman excitation profiles (REPs) for the representative 664, 793, 1314, and 1630 cm^{-1} modes are shown in Figure 3. Excitation profiles show the dependence of the Raman cross section on the excitation wavelength and were calculated based on the parameters used to fit the experimental absorption and Raman spectra of P_r in solution. The REPs of the 664 and 793 cm^{-1} bands show a single dominant band near the absorption maximum and a slight contribution at the 0–2 transition. As the vibrational frequency increases, the intensity in the 0–0 transition region decreases slightly and increases significantly in the 0–1 and 0–2 transition regions, as shown for the 1314 cm^{-1} and 1630 cm^{-1} REPs. The REPs show that the relative Raman intensities will change as a function of excitation wavelength and that pumping at an excitation wavelength closer to resonance would increase these intensities by 3 orders of magnitude. In our case, due to the significant fluorescence background from the P_r form, we pumped at a single frequency 2500 cm^{-1} to the red of the absorption maximum.

One important observation is the ratio of the absorption cross sections of the 0–0 and 0–1 vibronic transitions. In solution at 295 K this ratio is $A_{0-0}/A_{0-1} = 2.4$ (Figure 1A). If multiple species existed in the system, a change in temperature should shift the equilibrium, thus modifying the relative population of conformers and the resulting absorption spectrum. We see, however, that at 100 K the ratio of the vibronic transition strengths remains 2.4 (Figure 1B), further supporting a homogeneous system.

This observation is contrary to previous suggestions of a structurally heterogeneous population of phytochromes. The fluorescence data of 80 individual Agp1 phytochrome molecules at 100 K presented by Nieder and co-workers showed a series of single-molecule fluorescence emission spectra, each attributed to a different conformer.⁸ At low temperatures, however, excited molecules can photoconvert to different locally trapped intermediate states with unique absorption profiles, fluorescence spectra, and decay rates that may account for this heterogeneity.^{3,7}

Temperature dependent measurements of the P_r absorption profile of native PhyA revealed an isosbestic point, which was argued to

support the presence of two species in equilibrium.⁹ However, recent theoretical and experimental studies have shown that isosbestic points can exist in the inhomogeneously broadened spectra of a homogeneous system due to the slightly different local environments that individual solutes experience.²³ Furthermore, we have successfully modeled the P_r vibronic absorption profiles of phytochrome Cph1 as a function of temperature, including the thermal isosbestic point, by simply changing the temperature from 8 to 40 °C in the theory and adjusting the homogeneous contribution to the broadening (see SI Figure S3). Thus, the absorption isosbestic point does not provide definitive evidence for multiple P_r conformers, and we can conclude that Cph1's P_r absorption spectrum reflects a single predominant species in solution.

Acknowledgment. We thank Jon Hughes (University of Giesen) for the 100 K crystal absorption spectrum and Anne Myers Kelley (UC Merced) for the RRModel program. We also thank Lester Hedges for computational assistance. This work was supported by the Mathies Royalty Fund and supported in part by a grant from the National Institutes of Health (GM068552) to J.C.L.

Supporting Information Available: Additional experimental and computational details. This material is free of charge via the Internet at <http://pubs.acs.org>.

References

- (1) Rockwell, N. C.; Su, Y. S.; Lagarias, J. C. *Annu. Rev. Plant Biol.* **2006**, *57*, 837–858.
- (2) Quail, P. H. *Nat. Rev. Mol. Cell Biol.* **2002**, *3*, 85–93.
- (3) Dasgupta, J.; Frontiera, R. R.; Taylor, K. C.; Lagarias, J. C.; Mathies, R. A. *Proc. Natl. Acad. Sci. U.S.A.* **2009**, *106*, 1784–1789.
- (4) Schumann, C.; Groß, R.; Michael, N.; Lamparter, T.; Diller, R. *ChemPhysChem* **2007**, *8*, 1657–1663.
- (5) Heyne, K.; Herbst, J.; Stehlik, D.; Esteban, B.; Lamparter, T.; Hughes, J.; Diller, R. *Biophys. J.* **2002**, *82*, 1004–1016.
- (6) Müller, M. G.; Lindner, I.; Martin, I.; Gärtner, W.; Holzwarth, A. R. *Biophys. J.* **2008**, *94*, 4370–4382.
- (7) Holzwarth, A. R.; Venuti, E.; Braslavsky, S. E.; Schaffner, K. *Biochim. Biophys. Acta* **1992**, *1140*, 59–68.
- (8) Nieder, J. B.; Brecht, M.; Bittl, R. *J. Am. Chem. Soc.* **2009**, *131*, 69–71.
- (9) Schmidt, P.; Gensch, T.; Remberg, A.; Gärtner, W.; Braslavsky, S. E.; Schaffner, K. *Photochem. Photobiol.* **1998**, *68*, 754–761.
- (10) von Stetten, D.; Günther, M.; Scheerer, P.; Murgida, D. H.; Mroginski, M. A.; Krauß, N.; Lamparter, T.; Zhang, J.; Anstrom, D. M.; Vierstra, R. D.; Forest, K. T.; Hildebrandt, P. *Angew. Chem., Int. Ed.* **2008**, *47*, 4753–4755.
- (11) Lamparter, T.; Mittmann, F.; Gärtner, W.; Börner, T.; Hartmann, E.; Hughes, J. *Proc. Natl. Acad. Sci. U.S.A.* **1997**, *94*, 11792–11797.
- (12) Gambetta, G. A.; Lagarias, J. C. *Proc. Natl. Acad. Sci. U.S.A.* **2001**, *98*, 10566–10571.
- (13) Essen, L. O.; Mailliet, J.; Hughes, J. *Proc. Natl. Acad. Sci. U.S.A.* **2008**, *105*, 14709–14714.
- (14) McCamant, D. W.; Kukura, P.; Yoon, S.; Mathies, R. A. *Rev. Sci. Instrum.* **2004**, *75*, 4971–4980.
- (15) Myers, A. B.; Mathies, R. A. In *Biological Applications of Raman Spectroscopy*; Spiro, T. G., Ed.; John Wiley & Sons: New York, 1987; Vol. 2.
- (16) Lee, S. Y.; Heller, E. J. *J. Chem. Phys.* **1979**, *71*, 4777–4788.
- (17) Tang, J.; Albrecht, A. C. In *Raman Spectroscopy*; Plenum: New York, 1970; Vol. 2.
- (18) Lamparter, T.; Esteban, B.; Hughes, J. *Eur. J. Biochem.* **2001**, *268*, 4720–4730.
- (19) Matute, R. A.; Contreras, R.; Pérez-Hernández, G.; González, L. J. *Phys. Chem. B* **2008**, *112*, 16253–16256.
- (20) Borucki, B.; Otto, H.; Rottwinkel, G.; Hughes, J.; Heyn, M. P.; Lamparter, T. *Biochemistry* **2003**, *42*, 13684–13697.
- (21) Boitsov, V. M.; Yuzhakov, V. I. *J. Appl. Spectrosc.* **1986**, *45*, 1200–1203.
- (22) Mukamel, S. *Principles of Nonlinear Optical Spectroscopy*; Oxford University Press: New York, 1995.
- (23) Geissler, P. L. *J. Am. Chem. Soc.* **2005**, *127*, 14930–14935.

JA905822M